Food Chemistry 356 (2021) 129668

Contents lists available at ScienceDirect

Food Chemistry

journal homepage: www.elsevier.com/locate/foodchem

A fluorescence biosensor based on single-stranded DNA and carbon quantum dots for acrylamide detection

Qingyi Wei [a,b,c], Peiyao Zhang [a,b,c], Ting Liu [a,b,c], Hongbin Pu [a,b,c], Da-Wen Sun [a,b,c,d,*]

[a] School of Food Science and Engineering, South China University of Technology, Guangzhou 510641, China
[b] Academy of Contemporary Food Engineering, South China University of Technology, Guangzhou Higher Education Mega Center, Guangzhou 510006, China
[c] Engineering and Technological Research Centre of Guangdong Province on Intelligent Sensing and Process Control of Cold Chain Foods, & Guangdong Province Engineering Laboratory for Intelligent Cold Chain Logistics Equipment for Agricultural Products, Guangzhou Higher Education Mega Centre, Guangzhou 510006, China
[d] Food Refrigeration and Computerized Food Technology (FRCFT), Agriculture and Food Science Centre, University College Dublin, National University of Ireland, Belfield Dublin 4, Ireland

ARTICLE INFO

Keywords:
Acrylamide
Carbon quantum dots
Biosensor
Bread crust
DNA

ABSTRACT

As a potential carcinogen produced in food thermal processing, acrylamide (AM) can cause irreversible harm to human health. For the detection of AM in food products, a simple fluorescent biosensor based on single-stranded DNA (ssDNA) and carbon quantum dots (CQDs) was developed. Reduced fluorescence intensity of CQDs at 445 nm (excitation at 350 nm) was induced by the attachment of ssDNA. In the presence of AM, ssDNA was preferentially bound to AM by hydrogen bonding and the degree of fluorescence reduction was smaller than that without AM. Under optimized conditions, results showed that the sensing approach for detecting AM had a low detection limit of 2.41×10^{-8} M in the standard solution, and a linear relationship ranging from 5×10^{-3} to 1×10^{-7} M with the determination coefficient (R^2) of 0.9895 was obtained. Furthermore, a good recovery percentage (91.36–98.11%) in bread crust showed the potential for practical applications of this proposed biosensor.

1. Introduction

Acrylamide (AM), a white crystal substance mainly used to produce polyacrylamide, plays an important role in industrial production (Tan et al., 2019). However, this small molecular substance has been proved to have varying degrees of damage to human organs on the basis of its potential neurotoxicity (Tilson, 1981), genotoxicity (El-Assouli, 2009) and reproductive toxicity (Pundir, Yadav, & Chhillar, 2019). As early as 1994, the International Agency for Research on Cancer (IARC) of the World Health Organization included AM in the list of carcinogens in category II (World Health Organization, 1994). People can be exposed to AM through the skin, mucous membrane, respiratory tract and digestive tract, among which, diet is an important pathway of human contact with AM (Konings et al., 2003). AM is produced during food thermal processing, especially for processing foods rich in starch and protein (Hu et al., 2017), such as potato (15% of starch and 2% of protein) (El Sheikha & Ray, 2017) and crops including rice, sorghum and maize (8% of starch and 70% of protein) (Das, Adak, & Lahiri Majumder, 2020). For these raw materials, Maillard reaction easily occurs between amino compounds and reducing sugars in heating processes over 120 °C (Stadler et al., 2002), which produces melanoidins and flavor substances including reducing ketones, aldehydes and heterocyclic compounds, making food brown and fragrant. However, AM is also generated in large quantities as a by-product during Maillard reaction through the asparagine pathway (Tareke, Rydberg, Karlsson, Eriksson, & Törnqvist, 2002), posing a threat to human health. Therefore, it is particularly meaningful to establish a simple and sensitive method for the determination of acrylamide in food products.

Up to now, a lot of mature methods based on chromatography coupled with mass spectrometry have been used for the detection of AM. Lambert et al. (2018) analyzed the content of AM in 141 kinds of infant foods by using liquid chromatography coupled with mass spectrometry (LC-MS) instrument, confirming the reliability and versatility of the method. Sobhi, Ghambarian, Behbahani, and Esrafili (2017) developed an accurate and sensitive quantitative method of AM by gas chromatography-mass spectrometry (GC–MS), and the detection limit of

* Corresponding author at: School of Food Science and Engineering, South China University of Technology, Guangzhou 510641, China.
E-mail address: dawen.sun@ucd.ie (D.-W. Sun).
URL: http://www.ucd.ie/refrig, http://www.ucd.ie/sung (D.-W. Sun).

https://doi.org/10.1016/j.foodchem.2021.129668
Received 29 October 2020; Received in revised form 2 March 2021; Accepted 18 March 2021
Available online 23 March 2021

2 ng/L was obtained. Furthermore, Qin et al. (2017) developed a reliable detection method based on high-performance liquid chromatography-tandem mass spectrometry (HPLC-MS/MS) for simultaneous quantification of AM and 5-hydroxymethylfurfural (HMF) in seafood and showed satisfactory accuracy and precision of the method. However, these methods are difficult to detect the target directly in complex food systems, which require relatively complicated pretreatment processes, sophisticated instruments and time-consuming analytical procedures (Wu, Pu, Huang, & Sun, 2020; Hu, Sun, Pu, & Wei, 2020; Yaseen, Pu, & Sun, 2019). Therefore, for overcoming these problems, rapid detection methods based on the specific recognition of AM have been proposed, among which, biosensors composed of single-stranded DNA (ssDNA) or double-stranded DNA (dsDNA) have emerged (Jayan, Pu, & Sun, 2020; Zhou, Pu, & Sun, 2020). Li, Xu, Zhang, and Tong (2014) proposed a label-free electrochemical biosensor according to the interaction between AM and DNA immobilized on graphene oxide modified glassy carbon electrode and realized the sensitive and specific detection of AM. Similarly, fluorescent biosensors are also available by modifying biomolecules on fluorescent materials (Wang, Kong, Su, Liu, & Su, 2019). Asnaashari, Esmaeilzadeh Kenari, Farahmandfar, Taghdisi, and Abnous (2018) chose carboxyfluorescein (FAM) as the fluorescent substance and modified complementary strand DNA (csDNA) on it, which was then combined with ssDNA and gold nanoparticles for the quantitative sensing of AM. Other fluorescent materials including amino-CdSe/ZnS quantum dots (QDs) (Hu et al., 2014), Mn-doped ZnS QDs (Liu et al., 2018) and fluorescamine (Liu et al., 2014) had also been used to analyze the content of AM in foodstuffs. Besides, Wei, Liu, Pu, and Sun (2020a) also developed a fluorescence method for AM determination by adjusting the distance between the carbon quantum dots (CQDs), and satisfactory recoveries were realized when detecting AM in white bread crust samples. However, there is no report on applying CQDs and DNA as the fluorescent material and biological element in a fluorescent biosensor to determine AM in food products.

As a kind of fluorescent carbon nanoparticle with an average diameter below 10 nm, CQDs possess significant advantages including photostability, anti-photobleaching, low toxicity, water solubility and good biocompatibility (Lim, Shen, & Gao, 2015; Xu et al., 2004; Yang et al., 2018), and thus attract a lot of attention in the detection field (Qu, Wei, & Sun, 2018). In recent years, CQDs have demonstrated their ability and capability as fluorescence probes in detecting harmful residues and chemical substances, such as organophosphorus pesticides (Wu et al., 2017), chromogenic agent nitrite (Feng, Li, Zhang, Shi, & Zhou, 2017), heavy metal ions (Mashkani, Mehdinia, Jabbari, Bide, & Nabid, 2018; Xu, Wang, Li, & Zhao, 2020) and tea polyphenols (Wei, Liu, Pu, & Sun, 2020b). In addition, Cao et al. (2020) constructed a fluorescent resonant energy transfer (FRET) system by using CQDs labelled with DNA (pDNA) probe as the fluorescent donor, realizing the determination of microRNA-167 in *A. thaliana* seedlings.

Considering the outstanding characteristics of CQDs and the interaction of DNA with AM (Besaratinia & Pfeifer, 2007), this study aimed to develop a simple and sensitive biosensor for the rapid and reliable detection of AM. Specifically, group-rich CQDs were synthesized rapidly by one-step hydrothermal method and fluorescence of the CQDs was quenched by ssDNA due to its attachment. Upon the addition of AM, ssDNA was preferentially bound to AM by hydrogen bonding (Qiu, Qu, Dong, Ai, & Han, 2011), resulting in less free DNA, and the degree of fluorescence reduction was smaller than that without AM. Additionally, the practicability of this proposed method was confirmed by detecting AM in bread crust samples, which were prepared by QuECHERS (Quick, Easy, Cheap, Effective, Rugged and Safe) method (Wang, Sun, Pu, & Wei, 2019). For the first time, CQDs were applied to the detection of AM in a biosensor, which avoided complex modification and only needed simple preparation of CQDs and ssDNA solution. Apart from the simplicity and rapidity, the prepared biosensor also exhibited a wide detection range, a low detection limit, good reproducibility and high selectivity for AM detection.

2. Materials and methods

2.1. Chemicals and reagents

Citric acid, ethylenediamine, 6-aminocaproic acid (EACA), acrylic acid (AA), *n*-hexane and acetonitrile were purchased from Shanghai Macklin Biochemical Co., Ltd. (Shanghai, China). AM and 2-[4-(2-Hydroxyethyl)-1-piperazinyl]ethanesulfonic acid (HEPES) were obtained from Aladdin Reagent Co., Ltd. (Shanghai, China). Glycine (Gly), L-aspartic acid (L-Asp), sucrose (Suc) were supplied by Jingke Biotech Co., Ltd. (Guangzhou, China). QuECHERS pouches (including 150 mg $MgSO_4$, 50 mg primary secondary amine (PSA) and 50 mg HC-C18) were offered by Agilent Technologies Co. Ltd. (Shanghai, China). The ssDNA, 5′-ACG GCA ACA TGC CGA AGG AAC TAC CGG AAA CGG CAA ATC CTC G-3′ purified by UltraPAGE according to Asnaashari et al. (2018), was acquired from Sangon Biotech Co., Ltd. (Shanghai, China). All the reagents were analytically pure and no further purification was required. Ultrapure water prepared by a Milli-Q system (Millipore Co., Bedford, USA) was used during the whole experiment except double-distilled water (dd water) obtained from A.S. Watson Group Ltd. (Hong Kong, China) for the synthesis of CQDs.

2.2. Preparation and characterization of CQDs

Group-rich CQDs were synthesized by a one-step hydrothermal method according to Hou et al. (2013) with several modifications. In details, 20 mL of dd water was used to dissolve 2 g of citric acid and 1.043 mL of ethylenediamine. After mixing evenly, the solution was transferred into a high throughput closed microwave digestion/extraction workstation with twelve high-pressure reaction tanks (Jupiter-b, Sineo Microwave Chemistry Technology Co., Shanghai, China) and heated at 200 °C for 5 min. The preliminary CQDs product was obtained after the reaction temperature dropped to ambient temperature. Furthermore, the purification process was completed by firstly filtering the obtained solution with a microporous membrane (0.22 μm, Jinteng Experiment Equipment Co., Ltd., Tianjin, China), and then dialyzing the obtained filtrate with a dialyzer tube (MWCO, 100–500 Da, Shanghai Yuanye Biotechnology Co., Ltd., Shanghai, China) for 48 h. Finally, the resultant CQDs solution was dried by a freeze dryer (SCIENTZ-18 N, Xinzhi Bioscience Co., Inc., Ningbo, China) for 36 h, and the dried powder obtained was stored at 4 °C for later uses.

The transmission electron microscopy (TEM) image used to characterize the shape and size of CQDs was taken by a JEM-1400 Plus (JEOL Ltd., Tokyo, Japan) operating at 120 kV. The UV–vis absorption (Abs) of CQDs was measured through a UV–vis spectrophotometer (UV-1800, Shimadzu Co., Kyoto, Japan). The excitation (EX) spectrum and emission (EM) spectrum of CQDs were obtained by an RF-6000 fluorescence spectrophotometer (Shimadzu Co., Kyoto, Japan) equipped with a quartz carrier. The Fourier transform infrared (FTIR) spectrum of CQDs was acquired by a Tensor infrared spectrophotometer (Nicolet-iS50, Thermo Fisher Scientific Inc., Waltham, USA). The X-ray photoelectron spectroscopy (XPS) spectra of CQDs were acquired by an X-ray photoelectron spectrometer (Axis Ultra DLD, Kratos Analytical Ltd., Manchester, UK). The X-ray diffraction (XRD) pattern used to characterize the nanocrystal structure of CQDs was obtained by an X-ray diffractometer (D8 ADVANCE, Bruker Co., MA, USA), and the zeta potential of CQDs was measured using a potentiometric analyzer (Zetasizer Nano, Malvern Instruments Ltd., Melvin, UK).

2.3. Optimization of detection conditions

In order to acquire the required performance of the biosensor, the concentration of ssDNA and the incubation time of ssDNA and AM were optimized in the current study. For preparing the optimization experiments, synthesized CQDs powder was dissolved and diluted to 0.75 μg mL^{-1} with ultrapure water firstly, and ssDNA was dissolved into

solutions of different concentrations with HEPES buffer (pH 7.4).

For optimizing the concentration of ssDNA, 50 μL of ssDNA solutions with different concentrations of 0, 1.56, 3.125, 6.25, 12.5, 25 and 50 μM were added into 500 μL of diluted CQDs solution, and then ultrapure water was added to make the total volume of 600 μL. After mixing uniformly at 2800 rpm by a vortex mixer (MS3, Aika Instrument Co., Ltd., Staufen, Germany), the mixture was placed in a 37 °C water bath (HH-2, Changzhou Aohua Instrument Co., Ltd., Changzhou, China) to incubate for 45 min, and then the fluorescence spectra of the mixture were recorded by the fluorescence spectrophotometer under the following conditions: excitation wavelength of 350 nm, slit broadband of 3 nm, scanning range of 370–600 nm and scanning speed of 600 nm min^{-1}.

For optimizing the incubation time of ssDNA and AM, an amount of 50 μL of 12.5 μM ssDNA solution and 50 μL of 1×10^{-4} M AM standard solution dissolved in ultrapure water were added to 500 μL of diluted CQDs solution successively. After mixing uniformly by the vortex mixer, the mixture was incubated at 37 °C for 0–90 min, and then fluorescence intensities of the mixed solution were measured every 15 min by the fluorescence spectrophotometer with the same conditions detailed above.

2.4. Detection of AM in standard solutions

The detection of AM in standard solutions was performed as follows. Firstly, 50 μL of AM standard solution with different concentrations and 50 μL of 12.5 μM ssDNA solution were added into 500 μL of diluted CQDs solution, samples with final AM concentrations of 5×10^{-8}, 1×10^{-7}, 1×10^{-6}, 1×10^{-5}, 1×10^{-4}, 5×10^{-3}, 5×10^{-2}, 1×10^{-1} and 5×10^{-1} M were obtained. Subsequently, the samples were incubated at 37 °C for 45 min, and then fluorescence intensities were measured as described before.

2.5. Pretreatment of bread crust samples

Freshly baked bread samples were purchased in a local store (Guangzhou, China) and the QuECHERS method was utilized for sample pretreatment. First of all, 1 g dark brown bread crust was collected and ground, then the sample was added into 5 mL of hexane to remove the lipid. After being ultrasonically treated by an ultrasonic cleaning machine (SB-5200 DTDN, Xinzhi Biotech Co., Ltd., Ningbo, China) for 15 min, 5 mL of the mixed extractant composed of water and acetonitrile (v/v = 1:1) was added and oscillated through the vortex mixer for 10 min. Subsequently, the compound was centrifuged by a high-speed refrigerated centrifuge (Anhui Jiaven Equipment Industry Co., Ltd., Hefei, China) at 12,000 rpm for 20 min, and then the subnatant solution (acetonitrile phase) was moved to the QuECHERS pouch for oscillation purification for 10 min. Finally, the purified solution was centrifuged at 10,000 rpm for 10 min and ultrapure water was added to the collected supernatant until the final volume was 10 mL.

2.6. Detection of AM in real samples

The detection of AM in bread crust samples was performed as follows. The 10 mL of treatment solution for bread crust samples was filtered with the microporous membrane firstly. Then 25 μL of bread crust filtrate was spiked with 25 μL of AM standard solutions of different concentrations, and mixed with 50 μL of 12.5 μM ssDNA solutions, after that the mixture was added into 500 μL of diluted CQDs solution to make the final spiked concentrations of AM to 500, 50 and 5 μM, respectively. Subsequently, the mixture was incubated at 37 °C for 45 min, and fluorescence intensities were measured as described previously.

2.7. Statistical analysis

All measurements were conducted in triplicate and results were expressed as means ± standard deviation (He, Sun, Pu, & Huang, 2020). Origin 2019b software (OriginLab Co., MA, USA) was used for data processing and analysis. The particle size of CQDs in TEM images was measured by Nano_Measurer 1.2.5 software (Department of Chemistry, Fudan University, China). Besides, the limit of detection (LOD) was obtained through the following equation (Wei et al., 2020a):

$$\mathrm{LOD} = 3S_0 + Y_0 \quad (1)$$

where S_0 represents the standard deviation of the relative fluorescence intensity (ΔF) of blank solution at 445 nm, and Y_0 represents the mean ΔF of the blank solution.

3. Results and discussion

3.1. Sensing mechanism

The sensing mechanism of the proposed fluorescent biosensor is shown in Fig. 1. Firstly, the CQDs with rich groups on the surface were prepared by the one-step hydrothermal method with the assistance of microwave. With the addition of ssDNA as a biological recognition element to CQDs solution, functional groups such as amino and carboxyl groups on the surface of CQDs were covered by ssDNA, which was attached to CQDs through noncovalent interactions (Han et al., 2019; Luo et al., 2020), leading to a significant reduction in the fluorescence intensity of CQDs. Asnaashari et al. (2018) incubated the mixture of AM and ssDNA for 60 min, forming a strong binding interaction at the N-7 position of ssDNA. Likewise, with the adding of AM into the solution at the same time, a stable admixture was formed by AM and ssDNA through guanine bases due to their high affinity (Qiu, Qu, Dong, Ai, & Han, 2011), which reduced the concentration of free ssDNA in the solution. In such a situation, the fluorescence intensity of CQDs was higher than that without AM. According to the analysis of density functional theory (DFT), AM is not only a good hydrogen bond acceptor, but also a hydrogen bond donor of highly electronegative atoms such as O and N (Huang et al., 2016), which can form stable hydrogen bonds with purine and pyrimidine bases. Therefore, a stable admixture was formed by AM and ssDNA. Eventually, the quantitative detection of AM was realized by monitoring the change of emission peak intensity of CQDs at 445 nm induced by different AM additions.

3.2. Characterization of CQDs

The morphology of CQDs was characterized by TEM. As displayed in Fig. 2A, the approximately spherical CQDs were uniformly distributed in solution, the inset of size distribution in Fig. 2A shows that the main diameter of CQDs was 3.05 nm and the average diameter was 3.1 nm. The FTIR spectrum was used to indicate the surface group of CQDs, as shown in Fig. 2B, the strong and broad band distributed around 3250 cm^{-1} indicated the stretching vibrations of N—H and O—H (Feng et al., 2017; Wang et al., 2018). In addition, the peaks at 1644 cm^{-1} and 1268 cm^{-1} could be attributed to stretching vibrations of C═O and C—N, and bending vibrations of N—H and –CH_2 appeared at 1562 cm^{-1} and 1386 cm^{-1}, respectively (Cai et al., 2015; Zhai et al., 2014; Zhou et al., 2019). The results proved the existence of multiple functional groups on the surface of CQDs. Further, Fig. 2C shows the elemental components of CQDs through the XPS pattern. There were three elements of carbon (C1s, 281 eV), nitrogen (N1s, 397 eV) and oxygen (O1s, 529 eV) in CQDs, with percentages of 73.10%, 10.31% and 16.69%, which coincided with the result reported by Feng et al. (2017) that the same three elements with different percentages appeared in synthesized *N*-CQDs. Specifically, Fig. 2D shows that the three peaks at 281.6, 283.9 and 285.2 eV in the C1s spectrum corresponded to C—C/C—H, C—N and C═O bonds, as reported by Dong et al. (2012), and the peaks at 396.7 eV as well as 398.1 eV appeared in the N1s spectra (Fig. 2E) were related to C—N and N—H bonds according to Fu et al. (2020), which further

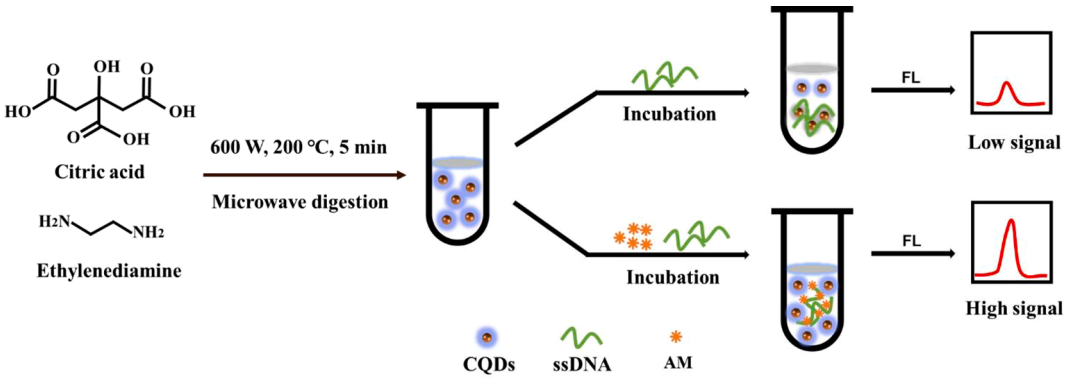

Fig. 1. Schematic representation of the AM determination based on the proposed fluorescent biosensor.

validated the results of FTIR. At the same time, the XRD pattern showed a strong diffraction peak located at $2\theta = 7.3°$ (Fig. 2F), which was related to highly disordered carbon atoms (Chen, Liu, Yang, Wang, & Zhuo, 2019), ulteriorly indicating the successful synthesis of CQDs.

The optical properties of CQDs were then studied. Fig. 2G shows the UV–vis absorption spectra and the fluorescence excitation and emission spectra of CQDs, indicating that the excitation and emission wavelengths of the highest fluorescence intensity were located at 350 nm and 445 nm, respectively. Correspondingly, the UV–vis of CQDs had an absorption peak at 350 nm, which was probably caused by n-π* transition of C═O bonds (Yue et al., 2016), and another absorption peak at 240 nm due to π-π* transition of aromatic sp^2 domains (Pan, Zhang, Li, & Wu, 2010). Cao et al. (2020) also synthesized CQDs with the same material and observed the optimal fluorescence excitation and emission wavelengths at 360 and 445 nm and two UV–vis absorption peaks at 245 and 357 nm, respectively. The little shift of the fluorescence and UV absorption peak positions in the two studies might be caused by the difference in the raw material dosages and heating methods. The photograph in the inset (left) of Fig. 2G shows a faint yellow colour of the prepared CQDs, and a blue fluorescence was present when CQDs were exposed to ultra-violet light at 365 nm as shown in the inset (right) of Fig. 2G. In addition, the fluorescence stability of CQDs was also one of the important factors in evaluating their applicability in the detection field. As displayed in Fig. 2H, when stored in a dark environment at 4 °C for 30 days, the CQDs also retained 94% fluorescence intensity of the new material, confirming their good stability. At the same time, continuous natural light had little effect on the fluorescence intensity of CQDs when stored at room temperature for 30 days, indicating the good anti-photobleaching property of CQDs.

3.3. Feasibility analysis for detecting AM

In order to verify the feasibility of the proposed biosensor, zeta potential analysis and fluorescence examination were carried out on three kinds of solutions of A, B and C, respectively, where solution A was single CQDs solution of 0.75 μg mL^{-1}, solution B was the mixture of 12.5 μM ssDNA solution and 0.75 μg mL^{-1} CQDs solution, which reacted at 37 °C for 60 min, and solution C was the mixture of 12.5 μM ssDNA solution and 1×10^{-4} M AM standard solution in CQDs solution (0.75 μg mL^{-1}) and reacted in the same conditions. The results of zeta potential measurement are shown in Fig. 3A with the relative standard deviation (RSD) from 2.09% to 4.03%, the zeta potential (-36.27 mV) of solution B was more negative than that of solution A (-27.53 mV) after attachment of ssDNA on CQDs, which was in line with the result shown by (Liu & Su, 2017), who synthesized $CuInS_2$ QDs with a negative zeta potential of −37.9 mV, and similarly obtained a more negative zeta potential of −45.0 mV after the attachment of ssDNA on $CuInS_2$ QDs. The reason for this phenomenon was that ssDNA was negatively charged (Zhai, Liu, Huang, Fang, & Zhao, 2017; Jiang, Sun, Pu, & Wei, 2019), which led to a lower zeta potential after reaction between ssDNA and CQDs or $CuInS_2$ QDs. However, when AM standard solution was added to the reaction solution at the same time, a stable admixture was formed by AM and ssDNA, which reduced the free ssDNA in the solution, thus resulting in an increase in the zeta potential (-30.14 mV) of solution C compared with solution B. The fluorescence examination results of the above solutions are displayed in Fig. 3B. Similar to the zeta potential results, the fluorescence intensity of solution B at 445 nm was lower than that of solutions C and A, which was caused by the fluorescence quenching effect of ssDNA to CQDs. Fig. 3B also shows the luminescence of the three solutions under an ultra-violet light at 365 nm, corresponding to the fluorescence spectra. Therefore, the fluorescent biosensor based on ssDNA and CQDs was able to quantify the detection of AM.

3.4. Optimization of detection conditions

In order to obtain the optimal concentration of ssDNA, a range of ssDNA solutions at different concentrations from 0 to 50 μM as shown from a to g in Fig. 3C were added into the diluted CQDs solutions for fluorescence testing, and the RSD obtained from three parallel samples were in the range of 0.90–1.38%. As shown in Fig. 3D, the fluorescence intensity of CQDs decreased significantly with increasing the concentration of ssDNA solution from 1.56 to 12.5 μM, which was ascribed to the coverage of the groups on the surface of CQDs by more ssDNA. Nevertheless, with a continuous increase of ssDNA solution concentration to 50 μM, the fluorescence intensity remained stable, which was probably due to that the amount of ssDNA covered on the surface of CQDs had reached saturation. Therefore, the minimum ssDNA concentration that could significantly reduce the fluorescence of CQDs was 12.5 μM, which was selected for the subsequent experiment.

For optimizing the incubation times of ssDNA and AM, the fluorescence intensities were measured in triplicate under incubation times from 0 to 90 min, with RSD from 0.78% to 2.38%. Fig. 3E compares the fluorescence intensities of the experimental group and the blank, in which the blank represented the sample without AM while the experimental group with AM. Results showed that as the reaction time increased from 0 to 45 min, the fluorescence intensities of both the experimental group and the blank gradually decreased, and then remained almost unchanged with the extending of the time to 90 min. As the free ssDNA could cover the surface of CQDs, a significant reduction in fluorescence intensity occurred under the condition of incubation at 37 °C for 45 min, while excessive time might affect the combination of AM and ssDNA according to Asnaashari et al. (2018). The ΔF (=F-F_0) was selected as the output signal, where F and F_0 represented the fluorescence intensities at 445 nm of the samples with and without AM. Fig. 3F shows that ΔF reached the maximum for the incubation time of 45 min, which was defined as the optimal reaction time for AM detection.

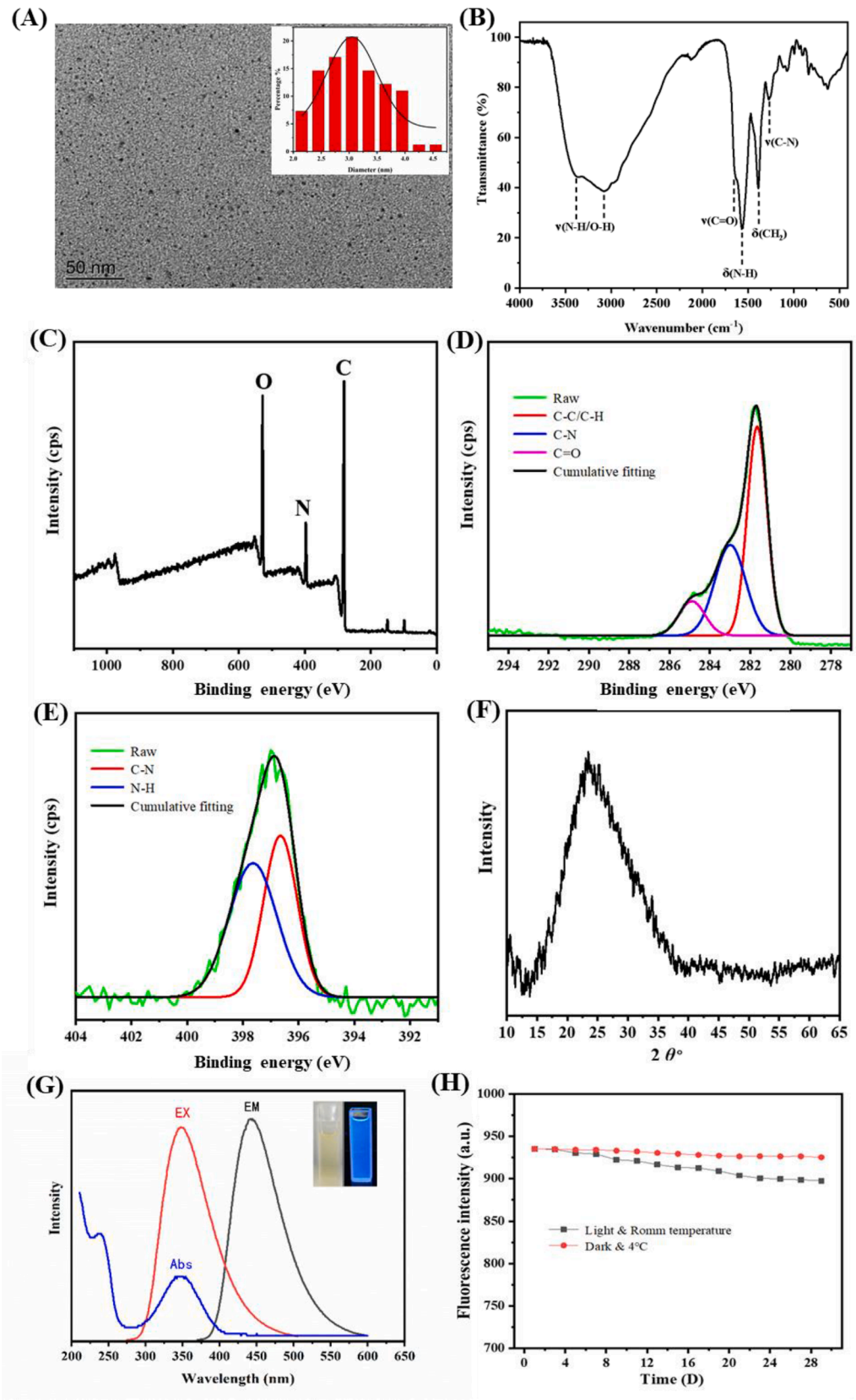

Fig. 2. Characterization of CQDs: (A) TEM image and the inset shows the particle size distribution of CQDs; (B) FTIR spectra; (C) XPS survey spectra; (D) C1s survey spectra; (E) N1s survey spectra; (F) XRD spectra; (G) The UV–vis absorption (Abs), excitation (EX) and emission (EM) spectra of CQDs, and the inset shows the photos of CQDs under daylight (left) and 365 nm ultra-violet light (right); (H) The Fluorescence stability under different storage environment. (For interpretation of the references to colour in this figure legend, the reader is referred to the web version of this article.)

3.5. Performance for detecting AM

Under optimized experimental conditions, the quantitative detection of AM was realized according to the change of fluorescence intensity at emission wavelength induced by various concentrations of AM. Fig. 4A displays the fluorescence spectra of the biosensor with AM concentrations from 1×10^{-7} to 5×10^{-3} M, which showed an increasing intensity relationship. With the single addition of ssDNA as a biological

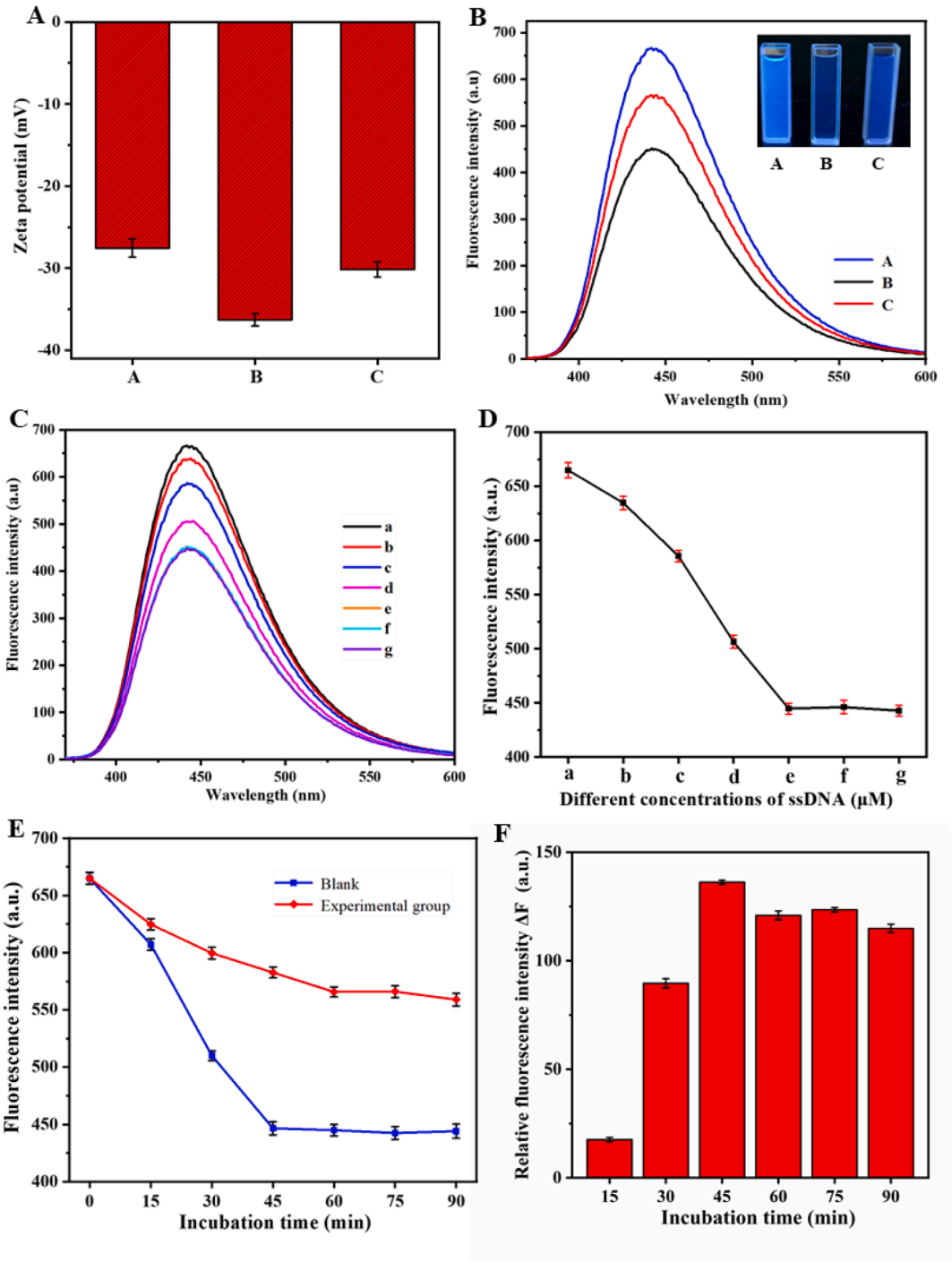

Fig. 3. (A) Zeta potential and (B) fluorescence spectra of solutions A, B and C, where A is CQDs solution (0.75 μg mL^{-1}), B is the mixture of ssDNA solution (12.5 μM) and CQDs solution (0.75 μg mL^{-1}), and C is the mixture of ssDNA solution (12.5 μM) and AM standard solution (1×10^{-4} M) in CQDs solution (0.75 μg mL^{-1}), and the inset image in (B) is the picture of solutions A, B and C under 365 nm UV light; (C) Fluorescence spectra and (D) fluorescence intensities of CQDs solution (0.75 μg mL^{-1}) with different concentrations of ssDNA (from a to g: 0, 1.56, 3.125, 6.25, 12.5, 25 and 50 μM) after incubation at 37 °C for 45 min; (E) Fluorescence intensities of blank (without AM) and experimental sample (with AM of 1×10^{-4} M) under different incubation times of 0, 15, 30, 45, 60, 75 and 90 min; (F) Relative fluorescence intensities (ΔF) of the sample under different incubation times, where $\Delta F = F\text{-}F_0$, F and F_0 are the fluorescence intensities of CQDs at 445 nm with and without AM.

recognition element to the sample, a significant reduction in the fluorescence intensity of CQDs occurred as expected. A similar phenomenon was also reported by Wang et al. (2019) that the fluorescence of CQDs with magnetic [GdCl3Br] counterions (CQDGd) was aggregation-induced quenched by ssDNA. On the addition of AM, ssDNA tended to form adducts with AM rather than adsorbed on the surface of CQDs, causing the fluorescence enhancement compared with CQDs-ssDNA solution (Besaratinia & Pfeifer, 2007). As shown in Fig. 4B, ΔF and the logarithmic AM concentration from 1×10^{-7} to 5×10^{-3} M followed a linear relationship of $\Delta F = 35.03 \times [\text{Log (AM concentration)}] + 284.67$ with the coefficient of determination (R^2) of 0.9895. The LOD was calculated to be 2.41×10^{-8} M. The error bars were the standard deviation calculated from the average fluorescence intensity of three parallel samples, and the obtained RSD were in the range of

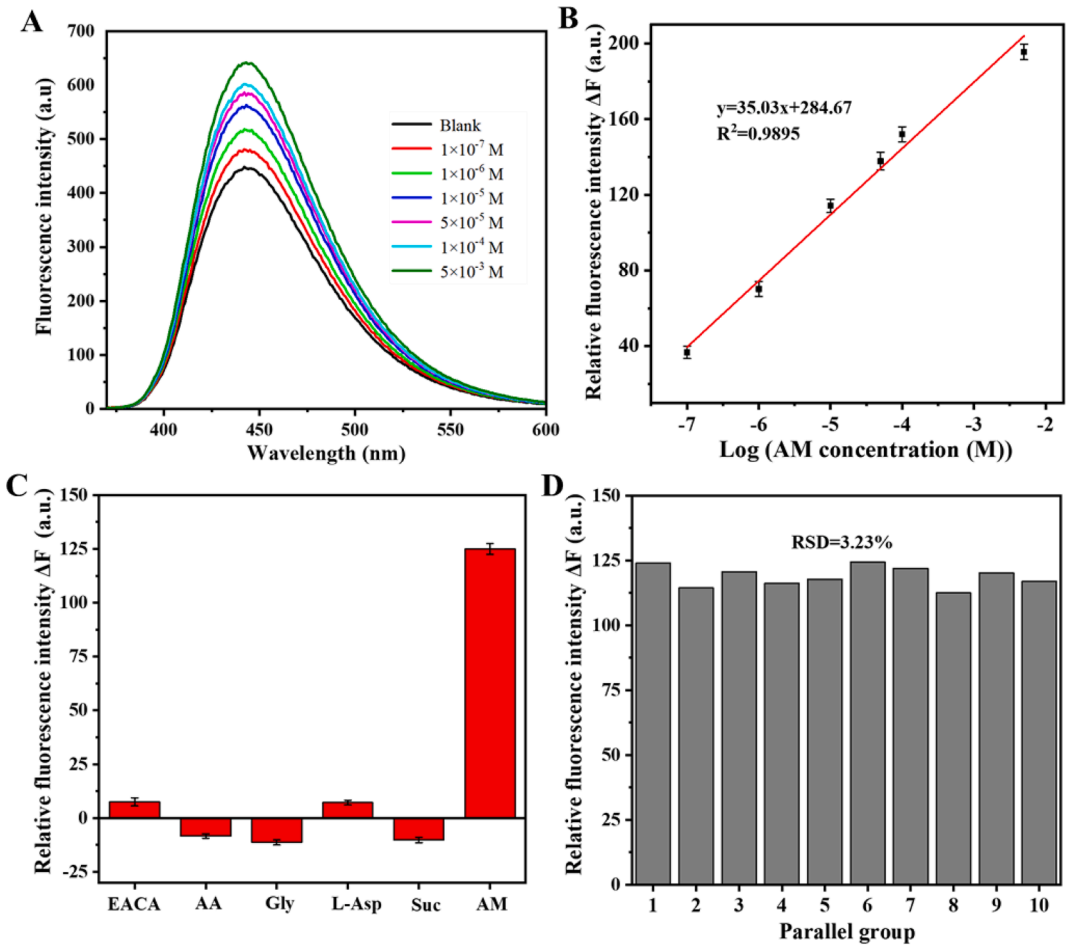

Fig. 4. (A) Fluorescence responses of CQDs with different concentrations of AM (1×10^{-7}, 1×10^{-6}, 1×10^{-5}, 5×10^{-5}, 1×10^{-4}, and 5×10^{-3} M) and blank (without AM); (B) Linear relationship between ΔF and the logarithmic AM concentrations; (C) ΔF of the samples under the presence of interfering materials of EACA, AA, Gly, L-Asp, Suc (1×10^{-3} M) and the target substance of AM (1×10^{-4} M); (D) ΔF of 10 parallel detection solutions.

0.63–0.81%. The results showed that the biosensor performed satisfactorily on the quantification of AM in the standard solution, which allowed the detection of AM with unknown concentrations.

Table 1 compares the detection performance of different sensors for AM quantification. Hu et al. (2014) and Wei et al. (2020a) successfully utilized the size-controlled fluorescence properties of CdSe/ZnS QDs and CQDs to quantify the detection of AM and obtained a LOD of 3.5×10^{-5} g L^{-1} (4.92×10^{-7} M) and 8.1×10^{-7} M, respectively. However, their processes were quite complicated and with many constraints, requiring the modification of *N*-acryloxysuccinimide on the surface of QDs and CQDs, and the polymerization reactions were triggered under heating or ultraviolet lamp irradiation with the existence of the initiator. Liu et al. (2018) designed a more complex method by combining a polymer imprinted with acrylamide (AM-MIP) and Mn(II)-doped ZnS QDs for detecting AM, which took more than 18 h on the single synthesis of AM-MIP, and the method showed a LOD of 1.7×10^{-7} M. In contrast, the current biosensor only required simple preparation of CQDs and ssDNA solutions, no complex modifications were needed to realize AM detecting, and a lower LOD of 2.41×10^{-8} M was obtained, which demonstrated the simplicity and high performance of the biosensor. It was also noteworthy that only 90 min was taken from the preparation of the solution to the detection of AM, which offered a more timesaving method

Table 1
Comparison of different sensors for AM detection.

Type of sensor	Detection range	LOD	Applicability	Reference
Fluorescent sensor based on gold nanoparticles and FAM-labeled double- stranded DNA	$0.05^{-1} \times 10^{-7}$ M	1×10^{-8} M	Potato fries water extract samples	Asnaashari et al. (2018)
Mn-doped ZnS quantum dots fluorescent sensor	0.5–60 μM	0.17 μM	Potato chips, fried bread stick, bread and rice crust	Liu et al. (2018)
Fluorescent sensor based on amino-CdSe/ZnS QDs	3.5×10^{-5}–3.5 g L^{-1}	3.5×10^{-5} g L^{-1}	Potato chips	Hu et al. (2014)
Fluorescent sensor based on CQDs	5×10^{-4}–5×10^{-6} M	8.1×10^{-7} M	White bread crust samples	Wei et al. (2020a)
Single-stranded DNA modified gold electrode	0.4–200 μM	8.1 nM	Tap water and potato crisps	Huang et al. (2016)
DNA Immobilized on Graphene Oxide-Modified Glassy Carbon Electrode	5×10^{-8}–1×10^{-3} M	Not mentioned	Tap water sample	Li et al. (2014)
HPLC-MS/MS	5.58–50.35 μg kg^{-1}	2.12 ng mL^{-1}	Thermally-processed seafoods	Qin et al. (2017)
GC–ECD	50–1000 ng L^{-1}	60.2 ng L^{-1}	Waste water	Sobhi et al. (2017)
Fluorescent biosensor based on CQDs and ssDNA	1×10^{-7}–5×10^{-3} M	2.41×10^{-8} M	Bread crust	This work

compared with traditional technology based on chromatography.

3.6. Specificity and reproducibility for AM detection

In order to evaluate the specificity of this biosensor, substances with a similar structure to AM, such as 6-amino-hexanic acid (EACA), acrylic acid (AA) and AM precursor substances like glycine (Gly), L-aspartic acid (L-ASP) and sucrose (Suc) were selected for interference examination. All the interfering substances with a concentration of 1×10^{-3} M and AM of 1×10^{-4} M were added into the ssDNA-CQDs reaction solution, respectively, and the results are shown in Fig. 4C with the RSD from 0.51% to 2.03%. The fluorescence intensities of CQDs at 445 nm were almost unchanged after adding the interfering substances, and their ΔF tended to zero or even negative, which were far lower than the fluorescence response after adding AM, indicating that these interfering substances could not combine with ssDNA to increase the fluorescence intensity of CQDs. Our results were consistent with the study reported by Asnaashari et al. (2018), who also showed that the response values of the selected interfering substances were significantly lower than that of AM, further proving the specificity of the biosensor based on ssDNA for AM detection. Furthermore, the reproducibility of the biosensor was investigated using 10 parallel ssDNA-CQDs solutions to detect AM with a concentration of 1×10^{-4} M, and Fig. 4D shows that the RSD obtained was 3.23%, indicating good reproducibility in detecting AM.

3.7. Application in real samples

For exploring the practical application of the constructed fluorescent biosensor in real samples, the determination of AM in bread crust was carried out. The bread crust was treated with *n*-hexane and the mixed extractant. Subsequently, the extract was purified by the QuECHERS method and filtered to obtain the treatment solution of bread crust samples, and spiked sample solutions with AM concentrations of 500, 50 and 5 μM were finally obtained after mixing different concentrations of AM standard solutions, ssDNA solution and CQDs solution in bread crust filtrate. Results in Table 2 shows that the recovery range of this detection biosensor was 91.36–98.11% with RSD of 1.15–2.30% (<5%), indicating the good accuracy and practicality of this biosensor.

Table 2
Practical application of the present biosensor for detection of AM in spiked bread crust samples.

Samples	Spiked concentration (μM)	Detected concentration (μM)	Recovery (%)	RSD (%)
1	500	490.53	98.11	1.15
2	50	45.68	91.36	1.96
3	5	4.71	94.20	2.30

4. Conclusions

In the current study, a simple and sensitive fluorescence biosensor for the determination of AM was proposed based on ssDNA and CQDs. The high affinity between ssDNA and AM as well as the excellent fluorescence properties of CQDs ensured the specificity and sensitivity of the biosensor. The established sensing biosensor offered a wide linear range for AM detecting from 1×10^{-7} to 5×10^{-3} M with a LOD of 2.41×10^{-8} M. Additionally, satisfactory recoveries ranging from 91.36% to 98.11% were obtained for detecting AM in bread crust samples prepared by the QuECHERS method, which further confirmed the practical application in AM contents monitoring of food products. Therefore, this fluorescence biosensor should have good potentials for sensing AM of other thermally processed foods with simplicity and sensitivity.

CRediT authorship contribution statement

Qingyi Wei: Supervision, Validation, Funding acquisition, Resources. **Peiyao Zhang:** Writing - original draft, Formal analysis, Investigation. **Ting Liu:** Formal analysis, Investigation. **Hongbin Pu:** Validation, Funding acquisition, Resources. **Da-Wen Sun:** Supervision, Funding acquisition, Resources, Writing - review & editing.

Declaration of Competing Interest

The authors declare that they have no known competing financial interests or personal relationships that could have appeared to influence the work reported in this paper.

Acknowledgements

The authors are grateful to the Guangdong Basic and Applied Basic Research Foundation (2020A1515010936) for its support. This research was also supported by the National Key R&D Program of China (2018YFC1603400), the Fundamental Research Funds for the Central Universities (D2190450), the Contemporary International Collaborative Research Centre of Guangdong Province on Food Innovative Processing and Intelligent Control (2019A050519001) and the Common Technical Innovation Team of Guangdong Province on Preservation and Logistics of Agricultural Products (2020KJ145).

References

Asnaashari, M., Esmaeilzadeh Kenari, R., Farahmandfar, R., Taghdisi, S. M., & Abnous, K. (2018). Fluorescence quenching biosensor for acrylamide detection in food products based on double-stranded DNA and gold nanoparticles. *Sensors and Actuators B: Chemical, 265*, 339–345.

Besaratinia, A., & Pfeifer, G. P. (2007). A review of mechanisms of acrylamide carcinogenicity. *Carcinogenesis, 28*(3), 519–528.

Cai, Q.-Y., Li, J., Ge, J., Zhang, L., Hu, Y.-L., Li, Z.-H., et al. (2015). A rapid fluorescence "switch-on" assay for glutathione detection by using carbon dots-MnO_2 nanocomposites. *Biosensors & Bioelectronics, 72*, 31–36.

Cao, X., Zhang, K., Yan, W., Xia, Z., He, S., Xu, X., et al. (2020). Calcium ion assisted fluorescence determination of microRNA-167 using carbon dots-labeled probe DNA and polydopamine-coated Fe_3O_4 nanoparticles. *Mikrochim Acta, 187*(4), 212.

Chen, Y.-J., Liu, Z.-E., Yang, Q., Wang, C.-F., & Zhuo, K.-L. (2019). Nitrogen-doped highly photoluminescent carbon dots derived from citric acid and guanidine carbonate. *Journal of Nanoscience and Nanotechnology, 19*(7), 4058–4063.

Das, P., Adak, S., & Lahiri Majumder, A. (2020). Genetic manipulation for improved nutritional quality in rice. *Frontiers in Genetics, 11*, 776.

Dong, Y., Wang, R., Li, H., Shao, J., Chi, Y., Lin, X., et al. (2012). Polyamine-functionalized carbon quantum dots for chemical sensing. *Carbon, 50*(8), 2810–2815.

El-Assouli, S. M. (2009). Acrylamide in selected foods and genotoxicity of their extracts. *The Journal of the Egyptian Public Health Association, 84*(3–4), 371–392.

El Sheikha, A. F., & Ray, R. C. (2017). Potential impacts of bioprocessing of sweet potato: Review. *Critical Reviews in Food Science and Nutrition, 57*(3), 455–471.

Feng, Z., Li, Z., Zhang, X., Shi, Y., & Zhou, N. (2017). Nitrogen-doped carbon quantum dots as fluorescent probes for sensitive and selective detection of nitrite. *Molecules, 22*(12), 2061.

Fu, Y., Wu, S., Zhou, H., Zhao, S., Lan, M., Huang, J., et al. (2020). Carbon dots and a CdTe quantum dot hybrid-based fluorometric probe for spermine detection. *Industrial & Engineering Chemistry Research, 59*(4), 1723–1729.

Han, G., Zhao, J., Zhang, R., Tian, X., Liu, Z., Wang, A., et al. (2019). Membrane-penetrating carbon quantum dots for imaging nucleic acid structures in live organisms. *Angewandte Chemie International Edition, 58*(21), 7087–7091.

He, H., Sun, D. W., Pu, H., & Huang, L. (2020). Bridging Fe_3O_4@Au nanoflowers and Au@Ag nanospheres with aptamer for ultrasensitive SERS detection of aflatoxin B1. *Food Chemistry, 324*, Article 126832.

Hou, J., Yan, J., Zhao, Q., Li, Y., Ding, H., & Ding, L. (2013). A novel one-pot route for large-scale preparation of highly photoluminescent carbon quantum dots powders. *Nanoscale, 5*(20), 9558–9561.

Hu, F., Jin, S. Q., Zhu, B. Q., Chen, W. Q., Wang, X. Y., Liu, Z., et al. (2017). Acrylamide in thermal-processed carbohydrate-rich foods from Chinese market. *Food Additives & Contaminants Part B-Surveillance, 10*(3), 228–232.

Hu, B., Sun, D.-W., Pu, H., & Wei, Q. (2020). Rapid nondestructive detection of mixed pesticides residues on fruit surface using SERS combined with self-modeling mixture analysis method. *Talanta, 217*, Article 120998.

Hu, Q., Xu, X., Li, Z., Zhang, Y., Wang, J., Fu, Y., et al. (2014). Detection of acrylamide in potato chips using a fluorescent sensing method based on acrylamide polymerization-induced distance increase between quantum dots. *Biosensors & Bioelectronics, 54*, 64–71.

Huang, S., Lu, S., Huang, C., Sheng, J., Zhang, L., Su, W., et al. (2016). An electrochemical biosensor based on single-stranded DNA modified gold electrode for acrylamide determination. *Sensors and Actuators B: Chemical, 224*, 22–30.

Jayan, H., Pu, H., & Sun, D.-W. (2020). Recent development in rapid detection techniques for microorganism activities in food matrices using bio-recognition: A review. *Trends in Food Science & Technology, 95*, 233–246.
Jiang, Y., Sun, D.-W., Pu, H., & Wei, Q. (2019). Ultrasensitive analysis of kanamycin residue in milk by SERS-based aptasensor. *Talanta, 197*, 151–158.
Konings, E. J., Baars, A. J., van Klaveren, J. D., Spanjer, M. C., Rensen, P. M., Hiemstra, M., et al. (2003). Acrylamide exposure from foods of the Dutch population and an assessment of the consequent risks. *Food and Chemical Toxicology, 41*(11), 1569–1579.
Lambert, M., Inthavong, C., Hommet, F., Leblanc, J. C., Hulin, M., & Guerin, T. (2018). Levels of acrylamide in foods included in 'the first French total diet study on infants and toddlers'. *Food Chemistry, 240*, 997–1004.
Li, D., Xu, Y., Zhang, L., & Tong, H. (2014). A label-free electrochemical biosensor for acrylamide based on DNA immobilized on graphene oxide-modified glassy carbon electrode. *International Journal of Electrochemical Science, 9*(12), 7217–7227.
Lim, S. Y., Shen, W., & Gao, Z. (2015). Carbon quantum dots and their applications. *Chemical Society Reviews, 44*(1), 362–381.
Liu, C., Luo, F., Chen, D., Qiu, B., Tang, X., Ke, H., et al. (2014). Fluorescence determination of acrylamide in heat-processed foods. *Talanta, 123*, 95–100.
Liu, Y., Hu, X., Bai, L., Jiang, Y., Qiu, J., Meng, M., et al. (2018). A molecularly imprinted polymer placed on the surface of graphene oxide and doped with Mn(II)-doped ZnS quantum dots for selective fluorometric determination of acrylamide. *Mikrochimica Acta, 185*(1), 48.
Liu, Z., & Su, X. (2017). A novel fluorescent DNA sensor for ultrasensitive detection of *Helicobacter pylori*. *Biosensors & Bioelectronics, 87*, 66–72.
Luo, X., Han, Y., Chen, X., Tang, W., Yue, T., & Li, Z. (2020). Carbon dots derived fluorescent nanosensors as versatile tools for food quality and safety assessment: A review. *Trends in Food Science & Technology, 95*, 149–161.
Mashkani, M., Mehdinia, A., Jabbari, A., Bide, Y., & Nabid, M. R. (2018). Preconcentration and extraction of lead ions in vegetable and water samples by N-doped carbon quantum dot conjugated with Fe_3O_4 as a green and facial adsorbent. *Food Chemistry, 239*, 1019–1026.
Pan, D., Zhang, J., Li, Z., & Wu, M. (2010). Hydrothermal route for cutting graphene sheets into blue-luminescent graphene quantum dots. *Advanced Materials, 22*(6), 734–738.
Pundir, C. S., Yadav, N., & Chhillar, A. K. (2019). Occurrence, synthesis, toxicity and detection methods for acrylamide determination in processed foods with special reference to biosensors: A review. *Trends in Food Science & Technology, 85*, 211–225.
Qin, L., Zhang, Y. Y., Xu, X. B., Wang, X. S., Liu, H. W., Zhou, D. Y., et al. (2017). Isotope dilution HPLC-MS/MS for simultaneous quantification of acrylamide and 5-hydroxymethylfurfural (HMF) in thermally processed seafood. *Food Chemistry, 232*, 633–638.
Qiu, Y., Qu, X., Dong, J., Ai, S., & Han, R. (2011). Electrochemical detection of DNA damage induced by acrylamide and its metabolite at the graphene-ionic liquid-Nafion modified pyrolytic graphite electrode. *Journal of Hazardous Materials, 190*(1–3), 480–485.
Qu, J., Wei, Q., & Sun, D.-W. (2018). Carbon dots: Principles and their applications in food quality and safety detection. *Critical Reviews in Food Science and Nutrition, 58*(14), 2466–2475.
Sobhi, H. R., Ghambarian, M., Behbahani, M., & Esrafili, A. (2017). Application of modified hollow fiber liquid phase microextraction in conjunction with chromatography-electron capture detection for quantification of acrylamide in waste water samples at ultra-trace levels. *Journal of Chromatography A, 1487*, 30–35.
Stadler, R. H., Blank, I., Varga, N., Robert, F., Hau, J., Guy, P. A., et al. (2002). Acrylamide from Maillard reaction products. *Nature, 419*(6906), 449–450.
Tan, X., Ye, J., Liu, W., Zhao, B., Shi, X., Zhang, C., et al. (2019). Acrylamide aggravates cognitive deficits at night period via the gut-brain axis by reprogramming the brain circadian clock. *Archives of Toxicology, 93*(2), 467–486.
Tareke, E., Rydberg, P., Karlsson, P., Eriksson, S., & Törnqvist, M. (2002). Analysis of acrylamide, a carcinogen formed in heated foodstuffs. *Journal of Agricultural and Food Chemistry, 50*(17), 4998–5006.
Tilson, H. A. (1981). The neurotoxicity of acrylamide: An overview. *Neurobehavioral Toxicology and Teratology, 3*(4), 445–461.
Wang, K., Sun, D.-W., Pu, H., & Wei, Q. (2019). Surface-enhanced Raman scattering of core-shell Au@Ag nanoparticles aggregates for rapid detection of difenoconazole in grapes. *Talanta, 191*, 449–456.
Wang, L., Wang, G., Wang, Y., Liu, H., Dong, S., & Hao, J. (2019). Fluorescent hybrid nanospheres induced by single-stranded DNA and magnetic carbon quantum dots. *New Journal of Chemistry, 43*(12), 4965–4974.
Wang, M., Kong, D., Su, D., Liu, Y., & Su, X. (2019). Ratio fluorescence analysis of T4 polynucleotide kinase activity based on the formation of a graphene quantum dot-copper nanocluster nanohybrid. *Nanoscale, 11*(29), 13903–13908.
Wang, X., Yu, S., Liu, W., Fu, L., Wang, Y., Li, J., et al. (2018). Molecular imprinting based hybrid ratiometric fluorescence sensor for the visual determination of bovine hemoglobin. *ACS Sensors, 3*(2), 378–385.
Wei, Q., Liu, T., Pu, H., & Sun, D.-W. (2020a). Determination of acrylamide in food products based on the fluorescence enhancement induced by distance increase between functionalized carbon quantum dots. *Talanta, 218*, Article 121152.
Wei, Q., Liu, T., Pu, H., & Sun, D.-W. (2020b). Development of a fluorescent microwave-assisted synthesized carbon dots/Cu^{2+} probe for rapid detection of tea polyphenols. *Journal of Food Process Engineering, 43*(7), Article e13419.
World Health Organization. (1994). Monographs on the evaluation of carcinogenic risks to humans. *Lyon, France: International Agency for Research on Cancer, 60*, 389.
Wu, L., Pu, H., Huang, L., & Sun, D.-W. (2020). Plasmonic nanoparticles on metal-organic framework: A versatile SERS platform for adsorptive detection of new coccine and orange II dyes in food. *Food Chemistry, 328*, Article 127105.
Wu, X., Song, Y., Yan, X., Zhu, C., Ma, Y., Du, D., et al. (2017). Carbon quantum dots as fluorescence resonance energy transfer sensors for organophosphate pesticides determination. *Biosensors & Bioelectronics, 94*, 292–297.
Xu, J., Wang, C., Li, H., & Zhao, W. (2020). Synthesis of green-emitting carbon quantum dots with double carbon sources and their application as a fluorescent probe for selective detection of Cu^{2+} ions. *RSC Advances, 10*(5), 2536–2544.
Xu, X. Y., Ray, R., Gu, Y. L., Ploehn, H. J., Gearheart, L., Raker, K., et al. (2004). Electrophoretic analysis and purification of fluorescent single-walled carbon nanotube fragments. *Journal of the American Chemical Society, 126*(40), 12736–12737.
Yang, Q., Li, J., Wang, X., Peng, H., Xiong, H., & Chen, L. (2018). Strategies of molecular imprinting-based fluorescence sensors for chemical and biological analysis. *Biosensors & Bioelectronics, 112*, 54–71.
Yaseen, T., Pu, H., & Sun, D.-W. (2019). Fabrication of silver-coated gold nanoparticles to simultaneously detect multi-class insecticide residues in peach with SERS technique. *Talanta, 196*, 537–545.
Yue, X., Zhu, W., Ma, S., Yu, S., Zhang, Y., Wang, J., et al. (2016). Highly sensitive and selective determination of tertiary butylhydroquinone in edible oils by competitive reaction induced "on-off-on" fluorescent switch. *Journal of Agricultural and Food Chemistry, 64*(3), 706–713.
Zhai, J., Liu, Y., Huang, S., Fang, S., & Zhao, M. (2017). A specific DNA-nanoprobe for tracking the activities of human apurinic/apyrimidinic endonuclease 1 in living cells. *Nucleic Acids Research, 45*(6), Article e45.
Zhai, Y., Zhu, Z., Zhu, C., Ren, J., Wang, E., & Dong, S. (2014). Multifunctional water-soluble luminescent carbon dots for imaging and Hg^{2+} sensing. *Journal of Materials Chemistry B, 2*(40), 6995–6999.
Zhou, X., Pu, H., & Sun, D. W. (2020). DNA functionalized metal and metal oxide nanoparticles: principles and recent advances in food safety detection. *Critical Reviews in Food Science and Nutrition, 1–20*. https://doi.org/10.1080/10408398.2020.1809343.
Zhou, X., Zhao, G., Tan, X., Qian, X., Zhang, T., Gui, J., et al. (2019). Nitrogen-doped carbon dots with high quantum yield for colorimetric and fluorometric detection of ferric ions and in a fluorescent ink. *Mikrochim Acta, 186*(2), 67.